

A NEW MODELING APPROACH FOR THE ASSESSMENT OF THE EFFECT OF SOLAR RADIATION ON INDOOR THERMAL COMFORT

Andrea Zani^{1,2}, Andrea G. Mainini¹, Juan D. Blanco Cadena¹, Stefano Schiavon², Edward Arens²

¹Politecnico di Milano, ABC Department, Milano, IT

²Center of the Built Environment, University of California, Berkeley, CA, USA

ABSTRACT

Thermal-comfort modeling has traditionally incorporated radiant effects via the metrics mean radiant temperature (MRT) and radiant temperature asymmetry. These metrics have not until recently, considered the effect of incoming solar radiation directly heating the occupants, though it significantly affects their thermal comfort.

In this paper, we describe a new approach for the calculation of the hourly effective radiant field (ERF) and mean radiant temperature (MRT) for an occupant near various façade systems and office layouts. The new method uses *Radiance* to assess the hourly intensity of solar radiation that passes through a facade and lands on the human body. The proposed method, for commercial buildings, allows calculating with high accuracy the comfort effect of solar radiation on occupants throughout the year.

INTRODUCTION

Indoor thermal comfort is one of the important design issues. Thermal comfort affects occupants' well-being, productivity and learning capability (Foda et al. 2011). A great deal of energy is consumed in buildings to maintain comfortable conditions.

Thermal comfort is hard to predict accurately and model in the design phase. It is determined by a variety of correlated variables that must be assessed together. The scientific community and professional standards have provided different methods, models, and tools to evaluate and predict building occupants' comfort. These are typically heat balance models assessing the air temperature (averaged over three heights representing the body), the humidity, the air speed, and various measures of radiant input such as the mean radiant temperature or radiant temperature asymmetry. Recently the solar radiation intensity impinging on the occupant has also been introduced into comfort analysis. The heat balance results are expressed as a Predicted Mean Vote (PMV), representing the thermal sensation of a population of occupants in a given set of condition. PMV can be accumulated to obtain the total amount of discomfort hours during the year. In the past, the

accuracy of comfort models as used in design has been low compared to surveyed results from operating buildings. Some of this was due to the lack of analysis of solar effects in building perimeter zones.

Solar radiation incidence, in the form of direct, diffuse and indoor-reflected components, is responsible for: localized temperature rise in a given environment, which requires difficult and energy-intensive HVAC response, and the risk of overcooling from attempting to compensate for the strong local heat gains in sunlit areas (Arens et al. 2015; Marino et al. 2017). Solar radiation affects the MRT and the thermal perception of the occupants. Very few approaches have included this effect (Arens et al. 2015; Marino et al. 2017). For example, the ISO7730 and CEN15251 standards and regulations do not mention shortwave solar radiation in their comfort prediction or evaluation procedure, even though this particular component of the total solar radiation indoors is often the most influential (Marino et al. 2017). Some papers have evaluated its effect on the indoor thermal environment and estimated the effect on the building energy consumption together with the overall thermal comfort of the occupants (Bessoudo et al. 2010; Marino et al. 2017). It is possible to predict the location on which the direct beam radiation will fall, including the condition under which the radiation falls directly on the occupant (most unfavorable condition).

More complex multisegment human thermoregulation models allow designers to predict the occupant's core and skin temperature (Foda et al. 2011). Skin temperatures can later be translated into local thermal sensation and comfort, either by analyzing the overall body's, or specific parts', skin temperature. Comfortable conditions are then determined using an equivalent temperature approach or with the University of California Berkeley (UCB) advanced thermal comfort model (Arens et al. 2015; Zhang et al. 2010; Huizenga et al. 2001). These models, and in particular the multi-segment models, are used in the automotive design. The models are complex and require specialized designers and tools.

ASHRAE 55-2017 includes two approaches for estimating, in a simple way, the comfort condition when direct beam solar radiation strikes the occupant. 1. Full

calculation of MRT based on the work of (Arens et al. 2015): computing and then summing up the long and short wave MRT as it is described in the Standard's Appendix C (MRT is a function of surrounding surfaces, fenestration system, occupant position and posture, solar position, body exposure, clothing insulation and air temperature); 2. Assuming a MRT equal to 2.8 °C above the average air temperature, applicable only under certain prescribed conditions regarding air temperature stratification, active radiant surfaces, elements' U-value, maximum outside temperature, maximum window size and room space requirements.

The ASHRAE full calculation of MRT is included in the *SolarCal* module of the *CBE Thermal Comfort Tool* (Hoyt et al. 2017). A limitation of this approach is that designers need to assess the fraction of sky vault in view of the occupant, and the projected fraction of a representative person exposed to direct beam sunlight, especially for highly complex scenes. In addition, the current implemented method allows only point-in-time evaluations because the Standard's focus is on design conditions. This can lead to an incomplete understanding of the users' comfort conditions and of the effectiveness of the façade system to control incoming radiation during the entire year.

Although *Radiance* is mainly used to perform lighting and daylighting (Saxena et al. 2010), it has been used in many research projects to calculate incident solar radiation or solar heat gains (Fernandes et al. 2015), simply by using the entire solar spectrum in calculation and the solar material properties instead of those limited to the visible spectrum. *Radiance*, in comparison with programs such as *EnergyPlus* which uses simplified algorithms to assess the amount and the distribution of solar radiation distribution through the window system (Fernandes et al. 2015, NREL 2017) can determine with higher accuracy the total incoming solar radiation.

Using *Radiance* as a ray trace tool coupled with the Daylight Coefficient method allows the intensity of total solar radiation landing on a specific object, surface or occupant (when its location is known or assumed) to be predicted. This would improve the estimation of the comfort of the users and the overall body core and skin temperatures. In this work, a new modeling approach is presented for predicting the variation on indoor thermal comfort of occupants which are exposed to direct solar radiation by computing the change on the MRT and the ERF based on the presence of sunlight on the occupant, the area exposed to direct solar radiation and intensity of solar radiation after being filtered through the fenestration system. Furthermore, we will present a validation comparing the new method with the current standard (ASHRAE 55-2017) and a series of additional analyses and features that can be obtained exploiting the

Radiance functions. Finally, the new method was tested calculating the ERF, adjusted MRT and PMV for five different complex fenestration systems. These would provide useful information to designers to evaluate the effectiveness of the different envelope, plant systems, and strategies to provide an optimum indoor environment to the building occupants by refining the computation of overall and localized comfort condition.

SIMULATION

The simulation workflow was divided into four main branches as shown in Figure 1. First, the manikin and the scene subject were created using *Rhinoceros* and *Grasshopper*. The scene and manikin, previously generated, were converted into Radiance format files. Second, these files were used to calculate the incident solar radiation on the manikin employing the 2-phase Radiance method. Third, the MRT was assessed for the specific user's position in the office space through *EnergyPlus*, without including short-wave radiation effects. Finally, coupling the results of radiation and thermal analysis, the adjusted MRT and the PMV are calculated along the entire year.

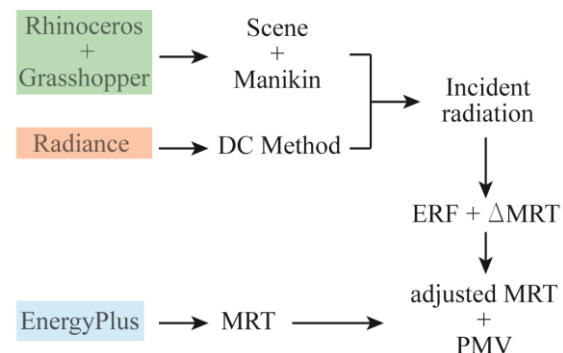


Figure 1 Simulation workflow

Radiance Daylight Coefficient method

The main change introduced in the new workflow in comparison with the standard method in ASHRAE 55 is the automated hourly calculation for the entire year of the incoming radiation falling on the user using *Radiance*. In particular, a modified version of the Daylight Coefficient (DC or 2-phase) method was selected (Figure 2). This method is able to consider the exact position of the sun, in contrast with the traditional method where the luminance of the sun is attributed to the three patches closest to the sun. In the proposed approach several Radiance programs are used, and minimal changes are applied to the traditional daylight workflow to enable modeling the incoming radiation landing on the manikin with high accuracy, even through a complex fenestration system (CFS). *Gendaymtx* tool generates a sky matrix with luminance values based on

direct and diffuse component of the solar radiation using the Perez distribution (Mardaljevic 1999). *Rfluxmtx* calculates the daylight matrixes taking into account sky conditions and scene characteristics. *Dcimestep* for the matrix multiplication and a modified version of *rmtxop* to obtain the irradiance [W/m^2] instead illuminance [Lux]. Irradiance values can be obtained integrating the luminance RGB radiance outputs for the entire solar spectrum.

The manikin is composed of 363 meshes wherein the centroid of each mesh a sensor point is placed, oriented with a normal outgoing to the centroid surface. Each sensor captures, for that specific portion of the body, the total solar radiation ($E_{solar,i}$) taking into account the diffuse, reflected and direct solar component. Multiplying the $E_{solar,i}$ for each mesh per their equivalent area and then adding each value, and finally dividing per total body area is possible to calculate hourly the incoming radiation for the whole body (E_{solar}) (W/m^2).

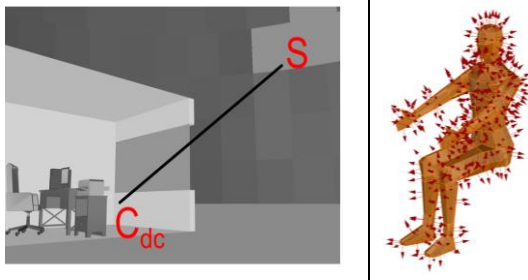


Figure 2 Radiance DC method representation (left)
Manikin meshes and vectors direction (right)

Using the formulas presented by (Arens et al. 2015) and hereby presented (1, 2), the effective radiant field (ERF) and the delta mean radiant temperature (ΔMRT) can be determined, representing the potential increment of MRT caused by solar radiation.

$$ERF = \frac{\alpha_{SW}}{\alpha_{LW}} E_{solar} \quad (1)$$

$$\Delta MRT = \frac{ERF}{f_{eff} h_r} \quad (2)$$

Where α_{SW} is the short-wave absorptivity, α_{LW} is the long-wave absorptivity of the human body, f_{eff} is the fraction of the body surface exposed to radiation (Arens et al. 2015) and h_r is the radiation heat transfer coefficient. Coupling the indexes calculated through *Radiance*, in the first part of the workflow, with the *EnergyPlus* simulation results, makes it possible to assess the comfort condition of the user.

Mean Radiant Temperature Calculation

Simultaneously, an energy simulation using *EnergyPlus* was run, in order to calculate the air temperature, humidity and surface temperatures for the different façade configurations presented in Table 1. The accuracy of the results in comfort analysis is highly influenced by the actual position of the manikin “user” and its orientation toward the facade. For this reason, the MRT is computed considering the surface temperatures of walls, glazed surfaces and the corresponding view factor for the exact user position, employing the method described in (Mackey et al. 2017). Adding to the hourly MRT the hourly ΔMRT is possible to obtain the adjusted MRT, that takes into consideration the effects of both radiative and solar radiation. Finally, the PVM model is fed to assess the thermal comfort and the percentage of potentially dissatisfied people.

Test case scenario

The simulated model presents the same geometry of the ASHRAE BESTEST office space (Henninger et al. 2004), in order to have a standard model. An open space office, located in Milan, Italy, with dimensions of 8 m wide, 6 m deep, and an internal height of 3 m and two windows facing south with dimensions equal to 2 x 3 m. The surfaces’ thermal and optical properties are listed in Table 1. For the purpose of the study, the thermal properties of the building envelope have been changed. The thermal model of the office presents only one exterior wall and two glazed surfaces facing outdoor conditions, and all the other surfaces are considered adjacent to offices with the same temperature. In order to guarantee a thermally neutral starting condition, an ideal HVAC has been considered with a $T_{heating} = 20^\circ\text{C}$, $T_{cooling} = 26^\circ\text{C}$ and minimum relative humidity equal to 30%. For the assessment of the PMV, and under mechanically controlled indoor conditions, the following standard values were used during the year: air flow speed 0.1 m/s, users’ metabolic rate of 1.2 met and a dynamic clothing level based on outdoor temperature (Schiavon et al. 2013). This last value is assumed in accordance with the office building use. As shown in Table 1, the influence of various façade configurations on users’ comfort was evaluated. Starting from a classic insulated glass unit (IGU) with a $T_{sol} = 0.6$ ($g=0.62$), three different shading systems were added, overhang, overhang plus shade fins and static louvers. In the final case, the standard IGU is substituted with solar control glass with a $T_{sol} = 0.28$ ($g=0.31$). Internal shading systems to control glare phenomenon, like roller shades, were not considered in this study. Table 1 shows the different user’s positions and orientations that were assessed to comprehend the influence of the solar radiation on the comfort for a given layout distribution.

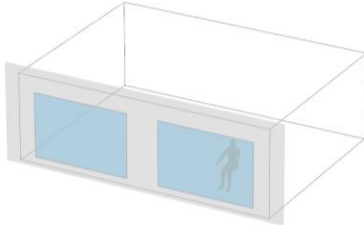
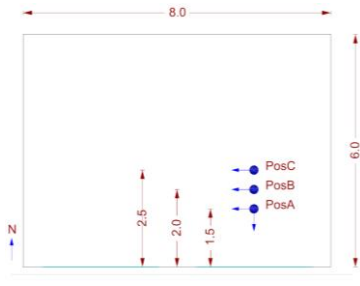
Case study – ASHRAE Bestest		Elements	$E+ (U_{value} - T_{sol})$	ρ
		Interior wall	Adiabatic	0.5
		Exterior wall	0.5	0.5
		Floor	Adiabatic	0.2
		Ceiling	Adiabatic	0.8
		Glazing ^(1,2)	$U = 1.4 \text{ W/m}^2\text{°C}$ $\alpha = 0.14^{(1)} - 0.35^{(2)}$ $T_{sol} = 0.6^{(1)} - 0.28^{(2)}$	
		Shading ⁽³⁾	-	0.6
Notes: Numbers (1,2) and (3) represent the different façade configurations in the case study. ⁽³⁾ Glazing (1) + External fixed louvers (spacing 45 cm – depth 45 cm). *Blue points indicate the user positions and the arrow body direction. ρ : Reflectance				

Table 1 Office space configuration (Bestest ASHRAE) and surface properties

VALIDATION

Radiance is widely used for the calculation of solar radiation, especially to determine solar heat gains for high-precision energy simulations. However, since the method presented in this paper is the first to use *Radiance* for the calculation of the ERF, it needs to be validated against appropriate method such as ASHRAE standard 55 appendix C. To prove the accuracy of the *Radiance* calculation under different sky condition (cloud coverage, irradiance value, and sun position) sunny and partially cloudy days near equinoxes and solstices were selected to compute point in time simulations of the ERF value. For the selected days, the ERF value was calculated following the procedure described in ASHRAE Standard 55 appendix C. As shown in the graphs in Figure 3, the coefficient of determination (R^2) for clear (a) and partially cloudy (b) days presents a strong fit, with respectively 0.95 and 0.97. The slight difference for the clear sky condition between 10 and 20 W/m² is given by the procedure used to calculate the sky vault view fraction (f_{svv}) or fraction of the body exposed to the sun (f_{bes}) for the ASHRAE method (less accurate due to a coarser sky patch).

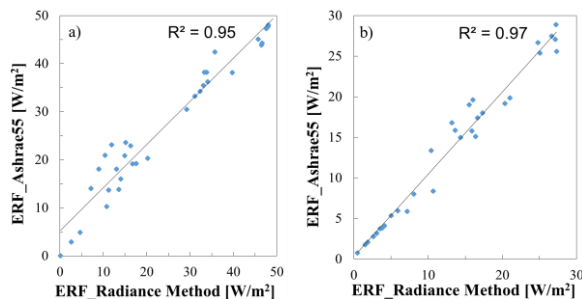


Figure 3 Comparison Radiance based-method and SolarCal CBE-ASHRAE a) Sunny sky, b) Partially Cloudy sky

Accordingly, this ray tracing method based on Radiance engine is sufficiently accurate for the stated application of the tool.

RADIANCE BASED-METHOD ADDITIONAL FEATURES

In this section, we present possible improvements that can be obtained using Radiance for the assessment of the incoming solar radiation on the human body, instead of using the approach of Standard55's Appendix C. The first one is a highly reliable method as proved in the validation, however difficult to implement in extensive explorations of different façade solutions over the entire year, especially in complex case studies and for CFS. Using the *Radiance* simulation engine based on raytracing calculation it is possible to estimate the radiation (direct + diffuse + reflected) without needing to calculate any geometrical quantities like sky vault view fraction (f_{svv}) or fraction of body exposed to sun (f_{bes}) (Fanger, 1970). These quantities can result in variable estimates depending on the interpretation of the designer especially for complex scene and fenestration system. Indeed, the real improvement of using *Radiance* is the possibility to obtain automatically those parameters throughout the year to generate an accurate hourly estimate of comfort related to solar radiation over time.

Furthermore, exploiting *Radiance* algorithms is possible to investigate the performance of several façade configurations like i.e. CFS (louvers, venetian blind (VB), and roller shade), electrochromic and fritted glass. In the next paragraphs, we present the additional features and output that the novel workflow is able to generate.

Detailed human body radiation map

As shown in Figure 4 a detailed hourly (or annual based on the time range of the output values) radiation map distribution on the body can be created. Each mesh of the manikin shows the point in time value of solar radiation [W/m^2] that hits the specific body part in function of the analyzed scene (interior layout, CFS and external context). This visualization can help the designer or the consultant to assess the most critical areas of the body for a specific design solution.

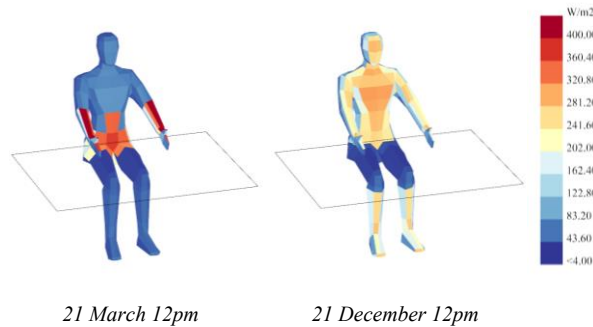


Figure 4 Radiation distribution on manikin surface

Furthermore, starting from the feature described in Figure 4, as well as from the visualization output, is possible to extract the amount of the body area [m^2] hit by direct radiation and the value of irradiance hour by hour for different body portions, like head, back, chest, etc.

A more detailed analysis, considering not only the influence of solar radiation on the entire surface of the body but also the different parts, can lead to more appropriate and accurate evaluations of the ERF index and the prediction of human local thermal sensation. For instance, the local E_{solar} values can be used to calculate ERF applying the appropriate value of short-wave absorptivity for each body part, based on the color of the skin and clothes (Lai et al. 2017) instead of the average value of α_{SW} equal to 0.67. As shown in Table 2 the variation between an ERF value calculated with average short-wave absorptivity and extreme values (light = white/beige outfit $\alpha_{\text{SW}} = 0.45$ and dark = black/ dark grey suit $\alpha_{\text{SW}} = 0.88$) can differ up to 25-30%.

	9	10	11	12	13	14	15
ERF α_{SWave}	20	34	45	46	48	33	10
ERF α_{SWdark}	27	45	61	62	64	44	14
ERF α_{SWlight}	14	22	29	30	31	21	7

Table 2 ERF hourly values for different clothing absorptivity

Furthermore, in future studies, it will be possible to investigate the effects of incoming solar radiation on the thermal sensitivity of each body parts and consequently the influence on the overall body thermal sensation based on CBE studies of whole-body sensation and comfort (Zhang et al. 2010). For instance, when direct radiation hits the head, being more sensitive to warmth, the whole-body thermal and comfort sensations tend toward uncomfortable levels.

Annual analysis

With Radiance it is possible to calculate, with a single simulation, the annual values of radiation and subsequently annual ERF and the change on MRT (ΔMRT). Comparing the heat maps in Figure 5 one can readily appreciate that the louvers solution can reduce the number of potential discomfort hours ($\Delta\text{MRT} > 4-5^\circ\text{C}$ causing a PMV variation between 0.5-0.7), while at the same time identifying critical conditions during the year. A detailed scene takes 10 min to run using one standard processor. Considering machine time and accuracy of the proposed method, this additional feature allows to easily assess the hourly annual comfort condition of the user in function of position in the space and façade system.

RESULTS AND ANALYSIS

We tested and analyzed 10 different direct solar radiation exposures during occupied hours, as described in Table 1. 3 locations (1.5, 2 and 2.5 m away from the window); 2 rotations, South (SS) and West (SW) oriented; and for the worst condition found, we tested 4 strategies (different glazing (labeled 60 and 28), shading louvers (L), and 2 types of overhangs (O and O2) aiming to control the disturbing effect caused. As indoor conditioning was done continuously through the year, the additional discomfort for the user would be caused by the increase of MRT due to shortwave radiation.

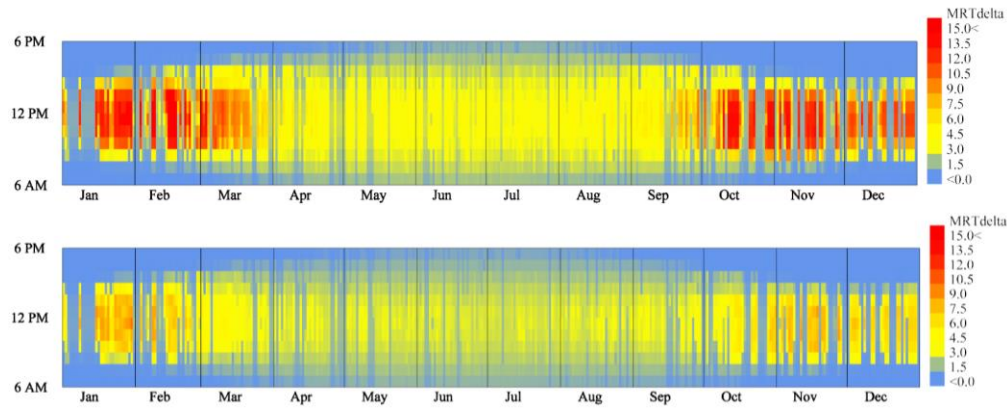


Figure 5 Heat map of Annual hourly ΔMRT ($^{\circ}C$): a) DGU $T_{sol}=60$ b) DGU $T_{sol}=60$ + Louvers

Assuming that the occupants would be in discomfort if the PMV values drop below -0.5 or rise above 0.5: a significant number of discomfort hours would occur for any of the exposures tested--1697 h (42%) and 2601 h (65%) were found to be the lowest, for standard PMV and corrected PMV (PMV_{adj}) values--whether the shortwave radiation effect was considered or not, as a result of the room overheated conditions. Nevertheless, the increment is considerable when the effect is included (from 7 to 23% of the total occupied hours, depending on the position, orientation and façade configuration). Large variations on the MRT were found, and they fluctuate considerably during the day, especially during midday (see Figure 7 and Figure 9); values of ΔMRT computed were as large as $23^{\circ}C$. The worst exposure condition (considering the ΔMRT) was found to be at 1.5 m from the southern window (POS A), looking towards west, especially on February 9th. This exposure condition (SW_60_1.5) suffered: 3301 (82%) discomfort hours, through the year; a maximum ΔMRT and PMV_{adj} of $23^{\circ}C$ and 4.14; an average ΔMRT and PMV_{adj} of $3.8^{\circ}C$ and 1.12. Figure 6 and Figure 8 present the variance of PMV and PMV_{adj} for the representative case studies to see the influence of shortwave radiation. Table 3 and Table 4 compile the number of discomfort hours (DH) computed for both PMV and PMV_{adj} , within the occupied hours (8:00 – 19:00), comparing their fluctuation due to either the occupant position or the façade configuration.

Influence of layout distribution on thermal stress

The location of the occupant in the room and the orientation of the body are sensitive to the values found for ΔMRT and PMV_{adj} . For the same body orientation (either South or West), the closer the manikin is to the window, the higher discomfort condition's frequency and intensity.

Case	PMV based		PMV _{adj} based	
	DH [h]	DH Ratio	DH [h]	DH Ratio
SS_60_1.5	2898	72 %	3247	81 %
SS_60_2	2921	73 %	3219	80 %
SS_60_2.5	2915	73 %	3181	79 %
SW_60_1.5	2898	72 %	3301	82 %
SW_60_2	2921	73 %	3267	81 %
SW_60_2.5	2915	73 %	3225	80 %

Table 3 Potential discomfort hours – layout distribution comparison

Assuming the manikin in three different positions (1.5, 2 and 2.5 m distant from the glass surfaces), we found that for every 0.5 m distance, there was a 1% difference in discomfort hours over the year. Furthermore, the orientation of the manikin also affects the results by modifying body exposure; when the manikin was oriented towards the West, the potential discomfort condition frequency and intensity increases; we found variations of 1-2% on discomfort hours depending on the manikin orientation.

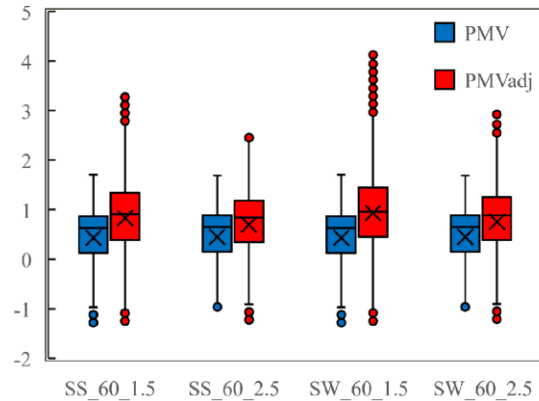
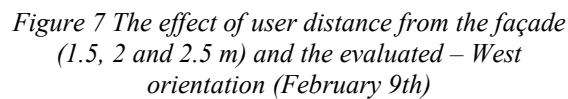


Figure 6 PMV and PMV_{adj} variance influenced by layout distribution

The results are mainly sensitive to the particular standardized geometry of the room considered, the characteristic of the building envelope materials, the average dimension of the glass portion of the façade, and the solar transmittance of the glass $T_{sol}=0.6$. The value of the (PMV_{adj}) is often higher than the maximum value acceptable of PMV . Extreme values exceeding $PMV = 3$ occur for 100 hours over the year (2.5% of the office hours).



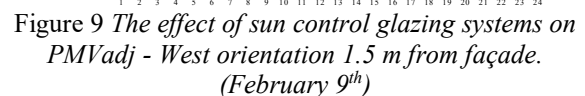
In addition, the variance on the thermal sensation after ΔMRT was considered, was reduced (see Figure 8 and Figure 9).

Table 4 *Potential discomfort hours – Façade comparison*

Box plot showing the distribution of PMV (blue) and PMVadj (red) values for three scenarios: SW_60_1.5, SW_60_1.5_O, and SW_28_1.5. The y-axis ranges from -2 to 5. The plot includes whiskers, boxes representing the interquartile range, a horizontal line for the median, and individual dots for outliers.

Scenario	PMV Median	PMVadj Median	PMV IQR (approx)	PMVadj IQR (approx)	PMV Whiskers (approx)	PMVadj Whiskers (approx)	PMV Outliers (approx)	PMVadj Outliers (approx)
SW_60_1.5	0.5	1.0	0.2 - 0.9	0.5 - 1.5	-1.2 - 1.8	-1.2 - 2.8	-1.2, -1.1	-1.2, -1.1, 3.0, 3.1, 3.2, 3.3, 3.4, 3.5, 3.6, 3.7, 3.8, 3.9, 4.0, 4.1, 4.2
SW_60_1.5_O	0.5	0.8	0.2 - 0.8	0.4 - 1.2	-1.2 - 1.7	-1.2 - 2.5	-1.2, -1.1	-1.2, -1.1, 2.5, 2.6, 2.7, 2.8, 2.9, 3.0, 3.1, 3.2, 3.3, 3.4, 3.5, 3.6, 3.7, 3.8, 3.9, 4.0
SW_28_1.5	0.2	0.5	-0.1 - 0.7	0.2 - 0.9	-1.2 - 1.2	-1.2 - 1.2	-1.2, -1.1	-1.2, -1.1, 2.0

— PMV_{Tsol=0.6} — PMV_{adj_Tsol=0.6}
 - - - PMV_{Tsol=0.28} - - - PMV_{adj_Tsol=0.28}



CONCLUSIONS

This novel approach has proven high accuracy (when validated with the models found in literature) which together with the short calculation time, the possibility of dealing with complex fenestration systems and room configurations, could become a preferred methodology for use in early building design stages and design performance evaluation. Furthermore, the approach allows the designer to predict more accurate thermal sensations of the occupants across the room at every hour of the year, just by simulating the desired position and rotation of the manikin. Although direct solar radiation falling on the user might occur only a few hours during the day, it can generate a significant MRT rise repeatedly occurring throughout the year. This may increase the discomfort hours experienced by the occupants, leading to unacceptable thermal comfort, decay of human health, and loss of productivity and learning proficiency.

REFERENCES

- Arens, E., Hoyt, T., Zhou, X., Huang, L., Zhang, H., & Schiavon, S. (2015). Modeling the comfort effects of short-wave solar radiation indoors. *Building and Environment*, 88, 3–9.
<https://doi.org/10.1016/j.buildenv.2014.09.004>
- Bessoudo, M., Tzempelikos, a., Athienitis, a. K., & Zmeureanu, R. (2010). Indoor thermal environmental conditions near glazed facades with shading devices - Part I: Experiments and building thermal model. *Building and Environment*, 45(11), 2506–2516.
<https://doi.org/10.1016/j.buildenv.2010.05.013>
- Fanger, P. O. (1970). Thermal comfort: analysis and applications in environmental engineering. New York: McGraw-Hill. Retrieved from <file://catalog.hathitrust.org/Record/001627231>
- Fernandes, L. L., Lee, E. S., McNeil, A., Jonsson, J. C., Noudui, T., Pang, X., & Hoffmann, S. (2015). Angular selective window systems: Assessment of technical potential for energy savings. *Energy and Buildings*, 90, 188–206.
<https://doi.org/10.1016/j.enbuild.2014.10.010>
- Foda, E., Almesri, I., Awbi, H. B., & Sirén, K. (2011). Models of human thermoregulation and the prediction of local and overall thermal sensations. *Building and Environment*, 46(10), 2023–2032.
<https://doi.org/10.1016/j.buildenv.2011.04.010>
- Henninger, R. H., & Witte, M. J. (2004). EnergyPlus testing with ANSI/ASHRAE standard 140-2001 (BESTEST). *U.S. Department of Energy*, 2001(EnergyPlus Version 1.2.0.029-June 2004).
- Hoyt T., Schiavon S., Piccioli A., Cheung T., Moon D., S. K. (2017). CBE Thermal Comfort Tool. Retrieved from <http://comfort.cbe.berkeley.edu/>
- Huizenga, C., Hui, Z., & Arens, E. (2001). A model of human physiology and comfort for assessing complex thermal environments. *Building and Environment*, 36(6), 691–699.
[https://doi.org/10.1016/S0360-1323\(00\)00061-5](https://doi.org/10.1016/S0360-1323(00)00061-5)
- Lai, D., Zhou, X., & Chen, Q. (2017). Measurements and predictions of the skin temperature of human subjects on outdoor environment. *Energy and Buildings*, 151, 476–486.
<https://doi.org/10.1016/j.enbuild.2017.07.009>
- Mackey C., Baranova V, Petermann L., M. A. (2017). Glazing and Winter Comfort Part 2 : An Advanced Tool for Complex Spatial and Temporal Conditions, 2317–2325.
- Mardaljevic, J. (1999). Sky Models for Lighting Simulation. In *Daylight Simulation: Validation, Sky Models and Daylight Coefficients* (pp. 163–209).
- Marino, C., Nucara, A., & Pietrafesa, M. (2017). Thermal comfort in indoor environment: Effect of the solar radiation on the radiant temperature asymmetry. *Solar Energy*, 144, 295–309.
<https://doi.org/10.1016/j.solener.2017.01.014>
- Marino, C., Nucara, A., Pietrafesa, M., & Polimeni, E. (2017). The effect of the short wave radiation and its reflected components on the mean radiant temperature: modelling and preliminary experimental results. *Journal of Building Engineering*, 9(November 2016), 42–51.
<https://doi.org/10.1016/j.jobte.2016.11.008>
- NREL. (2017). Climate, Sky and Solar/Shading Calculations. Retrieved from https://www.energyplus.net/sites/default/files/docs/site_v8.3.0/EngineeringReference/05-Climate/index.html#sky-radiance-model
- Saxena, M., Ward, G., Perry, T., Heschang, L., & Higa, R. (2010). Dynamic Radiance - Predicting Annual Daylighting with Variable Fenestration Optics using BSDF. *Proceedings of SimBuild*, 402–409. <https://doi.org/citeulike-article-id:10500157>
- Schiavon, S., & Lee, K. H. (2013). Dynamic predictive clothing insulation models based on outdoor air and indoor operative temperatures. *Building and Environment*, 59, 250–260.
<https://doi.org/10.1016/j.buildenv.2012.08.024>
- Zhang H, Arens E, Huizenga C, (2010). Thermal sensation and comfort models for non-uniform and transient environments, part III: Whole-body sensation and comfort. *Building and Environment*, 45(2), 399–410.
<https://doi.org/10.1016/j.buildenv.2013.11.004>